PUBLISHED ONLINE: 3 MAY 2016 | DOI: 10.1038/NPHYS3745
nature physics

Magnetic-confinement fusion

J. Ongena[1]*, R. Koch[1], R. Wolf[2] and H. Zohm[3]

Our modern society requires environmentally friendly solutions for energy production. Energy can be released not only from the fission of heavy nuclei but also from the fusion of light nuclei. Nuclear fusion is an important option for a clean and safe solution for our long-term energy needs. The extremely high temperatures required for the fusion reaction are routinely realized in several magnetic-fusion machines. Since the early 1990s, up to 16 MW of fusion power has been released in pulses of a few seconds, corresponding to a power multiplication close to break-even. Our understanding of the very complex behaviour of a magnetized plasma at temperatures between 150 and 200 million °C surrounded by cold walls has also advanced substantially. This steady progress has resulted in the construction of ITER, a fusion device with a planned fusion power output of 500 MW in pulses of 400 s. ITER should provide answers to remaining important questions on the integration of physics and technology, through a full-size demonstration of a tenfold power multiplication, and on nuclear safety aspects. Here we review the basic physics underlying magnetic fusion: past achievements, present efforts and the prospects for future production of electrical energy. We also discuss questions related to the safety, waste management and decommissioning of a future fusion power plant.

Without the energy from our Sun, the Earth would be a cold desert. The fusion of hydrogen into helium in the Sun's interior generates an enormous, steady heat flux. In the so-called proton–proton cycle (see Box 1), about 0.5% of the mass of hydrogen nuclei is converted into energy and radiation, and then diffused in space. In this way, about 4 million tonnes of the mass of the Sun is converted into heat and radiation every second. This process has been going on for billions of years, and astrophysicists estimate that this should go on for another few billions of years before the primary fuel of the Sun—hydrogen—is exhausted.

The proton–proton cycle is based on the weak interaction. Its very low reaction cross-section makes it impossible to use for any practical application on Earth. Fusion of protons in the Sun is possible only because of the extreme conditions in its centre: pressures and temperatures of about 150 billion bar and 15 million °C, caused by the gravitational forces from a mass that is about 330,000 times larger than that of the Earth. To realize fusion on Earth much higher reaction probabilities are needed—reactions between isotopes of hydrogen and helium have this property. The simplest of these, the so-called deuterium–tritium (DT) reaction (see Box 1), can be realized at temperatures around 150 million °C. Although this is ten times as hot as the centre of the Sun, such temperatures are nowadays routinely achieved on Earth in devices that use magnetic fields to confine the hot fuel, albeit at much lower density than in the interior of the Sun, and hence also at a much lower pressure (a few bar). In the largest of these devices, the Joint European Torus (JET) (https://www.euro-fusion.org/jet) in Culham, UK, the magnetic field sustains a large temperature gradient of more than 150 million °C over a distance of about 1.5 m. Compared to styrofoam used for insulating houses, the quality of the heat insulation by the magnetic field in a fusion reactor is about 10 times better, the insulating layer is about 10 times thicker, and the heat flux is tens of thousands times larger. Such a huge temperature gradient is precisely the main difficulty in fusion research, in particular because it induces large turbulence. It is the task of fusion scientists to keep this turbulence to a minimum.

Will the DT reaction produce energy in a future reactor on Earth? For a few decades scientists have mastered this reaction in a controlled way. In 1991, the first large-scale test of the DT reaction took place in JET and about 2 MW of fusion power was produced in a short pulse of about 2 s (ref. 1). Since then, several megawatts of fusion power have been produced in a controlled way in the fusion devices designed for running DT plasmas: JET in Europe and the Toroidal Fusion Test Reactor (TFTR), Princeton, US. However, up to now, the fusion power produced has been close to, but still less than, the heating power injected to heat the fusion fuel. To demonstrate the technical and scientific feasibility of fusion as a reliable source of energy, a device with higher performance is needed. This device is ITER (http://www.iter.org), at present under construction as a worldwide collaboration in Saint-Paul-lez-Durance, France—next to the French Alternative Energies and Atomic Energy Commission (CEA) Cadarache site.

Fusion material at temperatures of 150 million °C should obviously not come into contact with a material wall—otherwise the surface of the wall would melt or evaporate, and the released impurities would dilute and cool down the fusion material. Because, at such extremely high temperatures, hydrogen gas is transformed into a mix of independently moving positively charged ions and negatively charged electrons—the so-called plasma state—strong magnetic fields can be used to keep this plasma sufficiently far away from the wall. This is called 'magnetic confinement' and is discussed in detail below. Existing studies show that a magnetic-confinement fusion device with a volume between 1,000 and 1,500 m^3 (containing fusion fuel at only a millionth of the density of our atmosphere) would produce a thermal power of a few GW, resulting in an electric power of about 1 GW (ref. 2) using the conventional steam cycle.

Magnetic confinement

A charged particle in a strong magnetic field is bound to the magnetic field lines as a result of the Lorentz force. In a straight and uniform magnetic field, it follows a helical (corkscrew) path around a field line. This motion can be split into a circular motion, with a

[1]Laboratory for Plasma Physics, Royal Military Academy, Member of the Trilateral Euregio Cluster (TEC), Renaissancelaan 30, 1000 Brussels, Belgium. [2]Max-Planck Institut für Plasmaphysik, Wendelsteinstrasse 1, 17491 Greifswald, Germany. [3]Max-Planck Institut für Plasmaphysik, Boltzmannstraße 2, 85748 Garching bei München, Germany. *e-mail: j.ongena@fz-juelich.de

Box 1 | Fusion reactions.

The basic nuclear fusion reaction taking place in the Sun is the conversion of two protons into a deuteron (D):

$$p + p \rightarrow D + e^+ + \nu + 0.42\,\text{MeV}$$

The conversion of a proton (p) into a neutron (n) taking place involves the weak interaction, resulting in the production of a positron (e^+) and a neutrino (ν). This is then immediately followed by the annihilation of the positron, resulting in two gamma-ray photons:

$$e^+ + e^- \rightarrow 2\gamma + 1.022\,\text{MeV}$$

The first reaction is the beginning of a series of reactions, most of them mediated by the strong interaction, which converts four protons into a helium (^{4}He) nucleus.

The least difficult fusion reaction to put to work in a reactor built on Earth is the deuteron–triton (DT) reaction, the conversion of a deuteron and a triton (T) into a helium nucleus and a neutron (n):

$$D + T \rightarrow {}^4\text{He}\ (3.5\,\text{MeV}) + n\ (14.1\,\text{MeV})$$

The fast ^{4}He nucleus produced by the reaction is called an α-particle. The maximum reactivity is obtained for temperatures around 150 million °C and decreases very quickly below or above this temperature. In addition to deuterium (heavy hydrogen), this reaction requires the other hydrogen isotope tritium (super-heavy hydrogen), consisting of two neutrons and one proton. This artificial isotope, with a half-life of about 12 years, will be produced in the reactor from lithium, exploiting the neutron produced in the DT reaction:

$$^6\text{Li} + n \rightarrow {}^4\text{He} + T + 4.78\,\text{MeV}$$

$$^7\text{Li} + n \rightarrow {}^4\text{He} + T + n - 2.47\,\text{MeV}$$

Therefore, the fuels for DT fusion reactions are deuterium, which is plentiful, as 1/6,000th of all water on Earth contains this atom, and lithium, widely available in rocks and oceans[91]. The ash from the DT reaction is atomic helium—after recombination of the α-particles with electrons. Only tiny amounts of fuel are needed to supply our energy needs: about 15 g of DT fuel suffices to produce all the electrical energy needed by one EU citizen for 80 years.

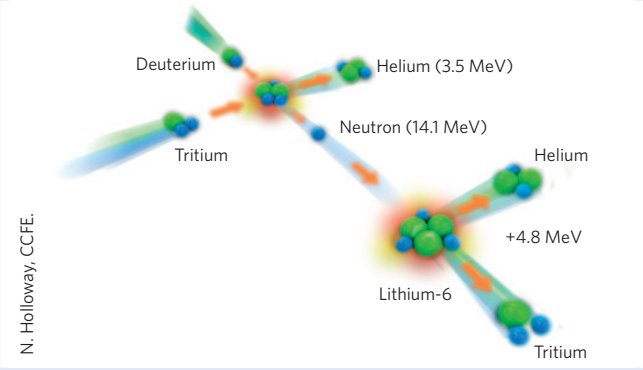

radius of gyration $r_L = v_\perp/\omega_c$ (also known as the Larmor radius) and a linear motion of the centre of the circle (the guiding centre), with a velocity $v_\parallel$ along the field line. $v_\perp$ is the component of the particle's velocity perpendicular to the direction of the magnetic field and $\omega_c = q_p B/m$ is the angular cyclotron frequency, with q_p the particle's charge, m the particle's mass and B the strength of the magnetic induction. As an electron is much lighter than an ion, it gyrates much faster (about two thousand times faster than a proton, ^{1}H, the nucleus of the lightest hydrogen isotope), but with a much smaller Larmor radius. In a fusion reactor, the magnetic field strength is chosen such that the ions' radii of gyration are much smaller than the dimensions of the device, for example, of the order of 10 mm, an electron's Larmor radius is then of the order of 0.1 mm. If the magnetic field is not uniform in space, the guiding centre drifts away from the magnetic field line, in opposite directions for ions and electrons (see Fig. 1).

The simplest magnetic field geometry one can think of for plasma confinement is that of a straight cylinder. However, this geometry has the problem that plasma particles escape at both ends. This escaping can be greatly reduced by forming two 'magnetic mirrors', which simply means that the field strength is increased at both ends using additional magnetic coils. Each charged particle can be seen as a tiny current loop (that is, a mini magnet) drifting along its guiding centre. The magnetic field of this magnet is always opposite to the externally applied field (that is, the particle behaves diamagnetically), and thus the particles always present an identical pole to that of the large magnetic coils at both ends. Because such magnets repel each other, plasma particles are repelled by the stronger end magnetic fields, and are thus contained within a 'magnetic bottle'. Machines based on this concept are called mirror machines. However, good confinement could never be achieved in such machines, mainly because of the instabilities generated by end losses. Indeed, the end mirrors do not reflect all particles, only those that have a sufficiently large perpendicular velocity component $v_\perp$ (that is, that are sufficiently strong mini magnets). Particles with a velocity directed mainly along the magnetic field line are not stopped by the end mirrors, and thus escape. Therefore, the particle population confined in the bottle is depleted in particles with small perpendicular velocity. Hence, the velocity distribution is non-maxwellian, which is a source of instabilities. The magnetic-mirror approach was finally abandoned in 1986 when the US decided not to operate the Mirror Fusion Test Facility B (MFTF-B) machine that was just ready for operation. (For a detailed history of fusion research up to around 2010 see refs 3–5.)

The obvious solution to prevent end losses is to wind the cylinder onto itself—in other words, to have a configuration with a toroidal shape. The necessary toroidal magnetic field is simply obtained by winding coils (toroidal field coils) around the toroidal vacuum chamber. However, such a system of coils generates a magnetic field that is stronger near the machine's vertical symmetry axis, because at that position the coils are much closer to each other than in the outer part of the torus. This causes a vertical drift of the particles that finally leads to charge build-up and plasma loss. This drift can be compensated—and all particles can be confined—if the magnetic field lines, instead of being circular as in the simple configuration just discussed, were wound around the torus in such a way that the drift in the outer part of the trajectory compensates that in the inner part (see Figs 1 and 2a). The 'amount of field-line winding' around the torus is called the rotational transform. After a certain number of turns around the torus, the field line has covered a surface, called the

NATURE PHYSICS DOI: 10.1038/NPHYS3745

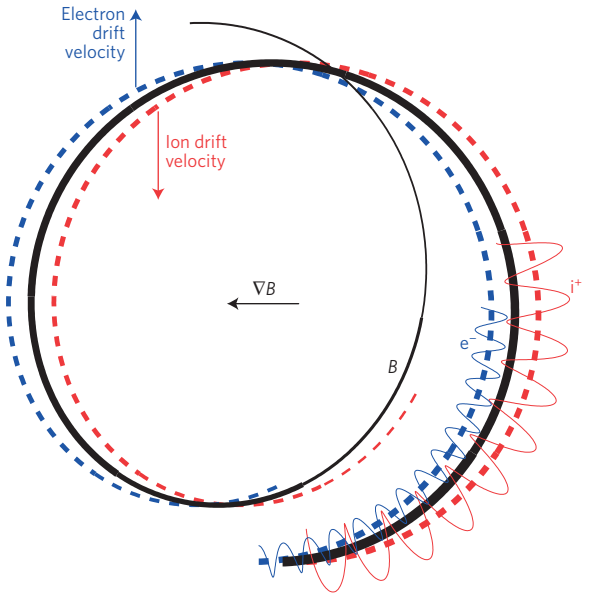

Figure 1 | Particle trajectory in a corkscrew-type magnetic field. The solid black line represents a magnetic-induction field line winding helically around a torus. (The magnetic induction B in vacuum is given by $B = \mu_0 H$, where H is the magnetic field and μ_0 the magnetic permeability of free space.) Because the magnetic field is non-uniform, the particle's guiding centre drifts away from the field line. The red and blue dashed lines represent an ion's and an electron's guiding-centre trajectories, respectively. The particle trajectories themselves, shown as solid wiggly coloured lines (ions 'i^+', electrons 'e^-') wind around the guiding centres (radii of gyration are not drawn to scale). Guiding centres drift away horizontally from the magnetic field line in one direction over half of the trajectory and in the opposite direction over the second half of the trajectory. The net result is a confined trajectory, displaced horizontally with respect to the field line (in one direction for ions and the opposite direction for electrons). The guiding-centre drift velocity causing this horizontal displacement is oriented vertically.

'magnetic surface'; every such surface is characterized by a winding number, called the safety factor q, equal to the number of turns the field line makes in the toroidal direction per turn in the cross-sectional, poloidal direction (see Fig. 2b).

Since the early days of fusion research, two alternative schemes have been in use to generate the rotational transform: the tokamak and the stellarator configurations. The tokamak configuration is shown in Fig. 2. The poloidal component of the magnetic field is generated by the toroidal current flowing in the plasma itself. The current is induced inductively, like in a transformer, by varying the magnetic flux in the primary (ohmic) transformer coils. This creates an inductive voltage (called the loop voltage) along the plasma torus (the secondary winding of the transformer), which drives the current in the plasma. As the plasma loop has electrical resistance, the current dissipates ohmic power that heats the plasma. For a large device with electron temperatures of several keV (tens of millions °C), typical loop voltages are of the order of one volt, with plasma currents up to several megaamperes and ohmic powers in the megawatt range. Additional coils (such as the vertical field coils in Fig. 2a) are also necessary to counteract the expansion forces of the plasma-current loop and of the plasma pressure, to shape the plasma or to create a divertor, a concept discussed below. The operation of a tokamak is pulsed by construction because the loop voltage must maintain the same sign to have a constant plasma current, so the primary current must constantly vary in the same direction from 'minus' the maximum technically possible current to 'plus' the same value; then the discharge must be terminated and the primary circuit of the transformer recharged for the next pulse. As discussed below, it is also possible to have stationary operation in a tokamak by inducing the electromotive force with waves or fast particles, or by exploiting thermo-electrical forces.

Continuous operation of a fusion device would be obtained in a simpler way if the need for a (pulsed) plasma current could be avoided. The stellarator concept provides such a solution; it relies on currents external to the plasma to create the helical magnetic configuration. In its basic configuration, extra helical coils around the toroidal plasma provide the necessary additional twist to the toroidal magnetic field generated by the main field coils. However, these helical windings around the plasma ring complicate the construction of a stellarator. Original stellarator configurations lacked good confinement properties. In modern stellarators, confinement has been optimized by means of a complex set of coils (see Fig. 3a). Several devices of the stellarator type are in operation or under construction at this moment. The largest optimized stellarator in Europe is Wendelstein 7-X (W7-X, (http://www.ipp.mpg.de/16900/w7x); see Fig. 3b) in Greifswald, Germany, which produced its first plasma on 10 December, 2015. A stellarator-like device (a so-called heliotron) of a similar size, the Large Helical Device (LHD, (http://www.lhd.nifs.ac.jp/en)) of the National Institute for Fusion Science (NIFS) near Nagoya, Japan, started operation in March 1998.

We should point out, however, that whereas the tokamak configuration has essentially undergone a selection process culminating in the ITER device and future demonstration (DEMO) reactor designs—that is, elongated plasmas with a poloidal divertor (see below) and a plasma aspect ratio $R/a \approx 3$, with R the major radius and a the minor radius of the torus—such convergence has not yet happened for stellarator designs, and hence meaningful comparisons between tokamaks and stellarators as fusion power plants still require a development process for the stellarator line of research. This will happen during the next decade or so using the devices mentioned above.

Particle and energy confinement

The race towards the generation of fusion power on Earth that started in the 1950s is largely a story of tokamak research[3–5]. Although the stellarator concept was never abandoned, the first large-size stellarator was put into operation in Japan only in 1998, well after the tokamaks TFTR and JET had produced megawatts of fusion power. Therefore, magnetic-fusion research is still strongly focused on tokamak development. With this in mind, we discuss in this section the physics of the tokamak approach to reactor-fusion plasmas.

One might think that the tokamak scheme has all the ingredients to reach fusion power production. Indeed, as heating is provided by the ohmic-heating power P_{OH} from the current that is induced inside the plasma, $P_{OH} = R_p I_p^2$ (R_p is the electrical resistance of the plasma torus and I_p the plasma current), it seems sufficient to increase the plasma current to a sufficiently high value to reach the necessary fusion temperatures (150 million °C). Unfortunately, physics limitations become important at this stage. The maximum plasma current I_p is not determined by technological constraints, but is limited by instabilities that destroy the plasma confinement whenever the safety factor q, characterizing the last magnetic surface confining the plasma, gets close to or below 2. This constraint leads to a maximum allowable value for the plasma current I_p for a tokamak operating at a given magnetic induction B_t. Indeed, the value of the safety factor is proportional to the ratio B_t/I_p, with the value of B_t being limited by the critical magnetic field of the superconductor and the mechanical forces arising in the coil assembly. Furthermore, the more the plasma is heated, the lower the

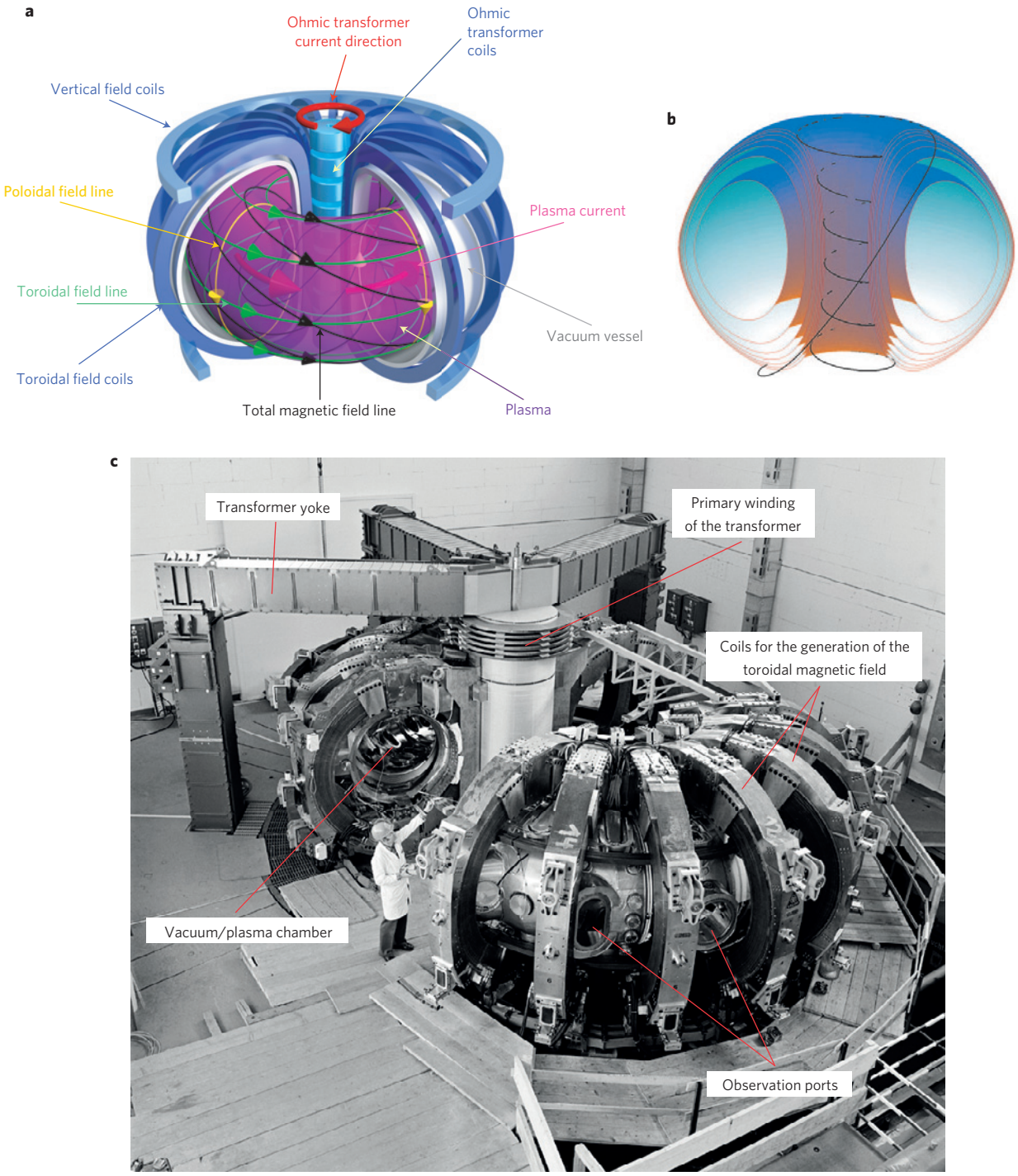

Figure 2 | Tokamak configuration and magnetic surfaces. a, A modern tokamak consists of a toroidally shaped vacuum vessel (with a D-shaped cross-section) around which coils are wound. Toroidal field coils 'wrapped around' the torus generate a toroidal magnetic field (green field lines). The current variation in the central ohmic transformer coils induces an electric field along these lines, which drives a toroidal flow for ions and electrons in opposite directions. This constitutes a current, the plasma current (big red arrows), which generates a poloidal magnetic field (yellow field lines). The superposition of the toroidal and poloidal field lines results in magnetic field lines winding around the torus, as shown in black, confining the charged plasma particles. Viewed as an electrical system, a tokamak is a transformer with ohmic transformer coils as the primary winding and the single-loop conducting plasma torus as the secondary winding. **b**, The total magnetic field lines describe so-called magnetic surfaces. One magnetic field line of the outermost magnetic surface is shown in black. It makes seven turns in the toroidal direction per turn in the poloidal direction, so this outer surface is characterized by a safety factor $q = 7$. Reproduced from ref. 100. **c**, Several essential elements of a tokamak are clearly visible on a picture of the (now dismantled) Tokamak Experiment for Technology Orientated Research (TEXTOR), Jülich, Germany, taken when the diagnostics and heating systems were not yet installed. Panel **a** courtesy of C. Brandt, IPP. Panel **b** reproduced from ref. 100, IOP. Panel **c** courtesy of M. Mangels, Forschungszentrum Jülich GmbH.

number of collisions between plasma particles, and so the lower the plasma's electrical resistance and hence the ohmic-heating power provided by the plasma current—it decreases proportionally with $T^{-3/2}$, where T is the plasma temperature.

NATURE PHYSICS DOI: 10.1038/NPHYS3745

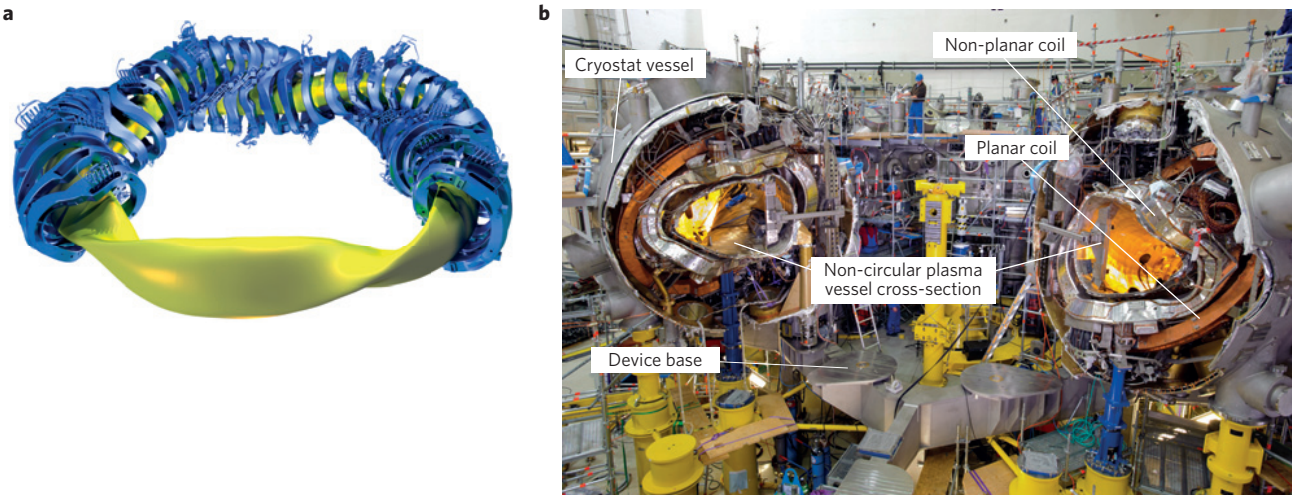

Figure 3 | W7-X optimized stellarator configuration. a, Schematic of the coil configuration and the surface of the confined plasma region. The modular coils are designed in such a way that they generate a specially tailored magnetic field that fulfils the theoretically calculated equilibrium, confinement and stability properties. **b**, Photograph of the device during the assembly process, illustrating the complex technical arrangement of the coils inside the cryostat vessel (just before the vessel was finally closed). Note the non-circular plasma cross-section with a shape depending on the position around the torus. Panel **a** courtesy of C. Brandt, IPP. Panel **b** courtesy of B. Kemnitz, IPP.

All in all, the pure tokamak scheme of operation alone cannot provide sufficiently high temperatures to generate large amounts of fusion power. To further increase the temperature of the plasma, additional heating methods must be used (see, for example, refs 6,7). One solution is the injection of fast particles. These must be neutral particles, otherwise they would be deflected owing to the Lorentz force in the strong magnetic field confining the plasma. A fast neutral particle crosses the magnetic field unimpeded, gets ionized by collisions with the plasma particles in the device, becomes part of the plasma, and then transfers its energy to the plasma. This heating scheme is called neutral-beam injection heating. Another way to heat the plasma is by injecting electromagnetic power. Owing to the Lorentz force, this will cause oscillations of the plasma particles. This coherent oscillation energy is then transferred to other plasma particles by random-kick collisions (thermalization). However, in a hot plasma, the number of collisions between particles is rather low, and therefore the transfer of energy is very inefficient unless the wave–particle interaction is amplified by a resonance. Choosing specific frequencies where the oscillations of the externally applied field are in resonance with the particle motion, such as the ion or electron cyclotron frequencies, leads to strong wave absorption and efficient plasma heating. These heating methods are collectively called auxiliary heating, as opposed to the intrinsic ohmic heating by the plasma current. Injecting a given total amount of heating power—that is, ohmic power plus auxiliary heating power, $P_{tot} = P_{OH} + P_{aux}$—one expects the total energy W of the plasma to increase at a rate $dW/dt = P_{tot} - W/\tau_E$, where the last term accounts for losses (by convection, conduction and radiation) characterized by τ_E, the so-called energy-confinement time. This is the characteristic time during which the plasma maintains its temperature if the heating power is suddenly switched off. This parameter is very important because to obtain a reactor-grade plasma, which should produce a very large amount of fusion reactions, it is not sufficient just to reach temperatures of about 150 million °C, as in addition the product of the number density of the ions n and the energy-confinement time has to satisfy $n_i\tau_E \geq 2 \times 10^{20}\,m^{-3}\,s^{-1}$. In other words, the plasma containing a sufficiently large number of reacting ions must stay hot for a long enough time to allow a sufficiently large number of fusion reactions to take place. The above inequality is a simplified version of the so-called Lawson criterion[8,9] that does not take into account engineering efficiencies. If this criterion is satisfied, the number of fast α-particles (energetic helium nuclei, ^{4}He, see Box 1) produced by the DT reaction is large enough to sustain the plasma temperature, much in the same way as external neutral-beam ions injected with an energy of 3.5 MeV would do. The plasma is then said to be ignited and the reaction becomes self-sustained. The reactivity of fusion plasmas is quantified by the power amplification factor (the fusion Q-factor) $Q = P_{fusion}/P_{tot}$. Two important landmarks for the value of Q are customary in fusion research. The first, break-even, is reached when the heating power is equal to the power produced from fusion reactions, corresponding to a $Q = 1$. The second, ignition, is reached when the additional heating systems can be switched off, corresponding to an infinite value for Q.

The first experiments with auxiliary heating systems were fairly disappointing: the confinement time was observed to decrease with increasing additional power ($\tau_E \propto 1/\sqrt{P_{tot}}$); in other words, the larger the injected power, the less efficient it becomes. This is because the transport is governed by turbulence driven by the strong gradients. Above a critical gradient, turbulence levels increase strongly, leading to the aforementioned decrease of confinement quality with heating power[10–12].

Moreover, problems were often encountered with impurity production when increasing auxiliary power. The use of the divertor concept, featuring an improved magnetic topology and a novel exhaust system (discussed in detail below), leading to a better separation between the hot plasma core and the colder edge plasma in contact with material surfaces, enabled the problem to be mitigated. Introduction of a divertor also led to an increase of the confinement time by a factor of two. It also uncovered an unexpected property of the plasma, namely that it allows bifurcated equilibria in the novel magnetic configuration. The improved confinement regime was called the H-mode ('H' for high confinement[13]), and since then, new plasma-confinement scenarios have been identified, called advanced modes, with additional special properties. Aside from confinement improvements, some of these modes enable a larger 'bootstrap current'—a self-generated current in the plasma due to thermo-electric effects, flowing in the same direction as the externally applied plasma current[14]. A large bootstrap current is mandatory to achieve steady state in the tokamak configuration (see below) owing to the limited efficiency of the auxiliary heating systems in driving the plasma current.

In recent decades, there have been substantial advances in understanding the role of turbulence in particle and energy transport across the plasma, confinement and bifurcation between different confinement modes. Confinement degradation is now understood on the basis of the 'anomalous' transport caused by turbulence. In the absence of turbulence, transport is due to collisions between plasma particles. Collisions displace particles from one trajectory to the next, leading to diffusion. The calculation of the diffusion coefficients taking into account the complex geometry of particle trajectories in a tokamak or a stellarator goes by the name of neoclassical transport theory (see, for example, ref. 15). If the transport were truly neoclassical, there would be no confinement degradation. Unfortunately, experiments have shown that the observed electron transport is about one order of magnitude larger than the neoclassical value. The anomalous transport is mainly due to electrostatic micro-turbulence driven by temperature gradients. This may take place both in the electron and ion channels, but the electron channel is the dominant one. Modelling of turbulence is a very complicated task owing to the very different timescales of electron and ion motions and the different spatial scales of turbulent structures[16]. The use of massively parallel computing in the past decade has enabled accurate modelling of these processes and reproduction of the experimental observations[17]—see, for example, figure 4 in ref. 16. It is nowadays possible to understand the interaction between the α-particle confinement in a reactor and the turbulence[18,19]. Recently, it has also become possible to simultaneously model electron and ion turbulence[20], considered a nearly impossible task just one decade ago.

The H-mode is now understood as resulting from the stabilization, by poloidally sheared flows, of unstable modes located in the vicinity of the last closed magnetic surface[21]. The quenching of anomalous transport in this region allows the existence of large pressure gradients, resulting in what is usually called a transport barrier.

In stellarators, neoclassical transport is a stronger contribution to heat loss than in tokamaks. Owing to the absence of axial symmetry, neoclassical transport scales very unfavourably with the plasma temperature, making this contribution a dominant part of the overall transport in the core of the plasma in stellarator configurations[22]. The magnetic-field configuration itself in stellarators also has an effect on plasma turbulence. For the optimized magnetic-field configuration of W7-X, profound effects on the turbulent transport are expected[23,24].

Plasma equilibrium and stability

As discussed in the previous sections, magnetic confinement of fusion plasmas is usually studied in a toroidal geometry. A good description of the force balance in a toroidal plasma is given by magnetohydrodynamic (MHD) theory, which is a hydrodynamic description that treats the plasma as an ideal gas with infinite electrical conductivity. This is a valid approach for high-temperature plasmas, as the electrical conductivity σ increases with electron temperature T_e ($\sigma \propto T_e^{3/2}$), and for timescales that are short with respect to a typical current-redistribution time. In particular, the ideal, stationary MHD force balance reads $\nabla p = \mathbf{j} \times \mathbf{B}$ and the magnetic equilibrium is found to be described very well by this relation (p is the plasma pressure, $\mathbf{j}$ the plasma-current density and $\mathbf{B}$ the magnetic induction). Linearizing the time-dependent ideal MHD equations, the stability of the system can be assessed. Large-scale MHD instabilities set important limitations to the operational range of fusion devices[25]. For both tokamaks and stellarators, the maximum achievable volume-averaged pressure is limited by the occurrence of ideal MHD instabilities when the ratio β between the plasma pressure and the pressure of the magnetic field, defined as $\beta = \langle p \rangle / (B^2/(2\mu_0))$, with $\langle p \rangle$ the average total pressure (the sum of the ion and electron pressures), exceeds a critical value of a few percent (the so-called β-limit)[26]. Including the effect of finite resistivity, it is found that, in tokamaks, the occurrence of so-called tearing modes can give rise to a slightly lower value of the β-limit. This is because tearing modes can lead to 'magnetic islands'—see Fig. 4. Magnetic islands are detrimental for the stability of the plasma, as they effectively short-circuit confinement by allowing heat and particles to flow rapidly across the plasma cross-section along the field lines in the island region, rather than by slow diffusion across flux surfaces. As mentioned above, the total value of the plasma current I_p in tokamaks is limited by the occurrence of ideal kink instabilities when the safety factor q drops below 1 (in practice, operation is already impossible at $q < 2$ unless active control of the kink instability is provided). This is important because both the energy-confinement time and the maximum density in a tokamak scale linearly with the plasma current[27]. Exceeding one of these limitations can cause a so-called disruption of the tokamak plasma, an event where, owing to the nonlinear interactions between several magnetic islands on different flux surfaces, the thermal insulation is lost on a timescale of a few hundred microseconds and the plasma current can no longer be sustained because of the strongly increasing electrical resistance as the temperature drops. Such events can generate large thermal and mechanical loads on the tokamak assembly, and hence have to be minimized in future large devices such as ITER. The stellarator, owing to the absence of a toroidal plasma current, does not face these problems—a big conceptual advantage.

It is worth noting that MHD instabilities are not always unwanted; in fact, they can also provide a self-limited operation

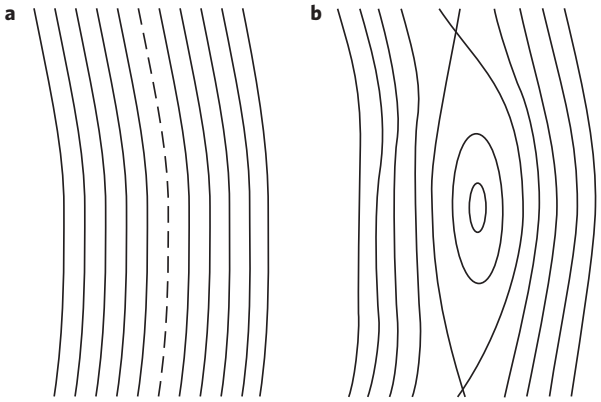

Figure 4 | Magnetic islands. If a magnetic surface is characterized by a rational winding number (in other words, the safety factor q is the ratio of an integral number of toroidal turns and an integral number of poloidal turns), it is called a rational magnetic surface. These surfaces are 'exceptional', in the sense that almost all surfaces are irrational, even though the set of rational numbers is 'dense' (in the mathematical sense) in the set of real numbers. For example, the unperturbed $q = 7$ surface shown in Fig. 2b is a rational surface. Such rational surfaces are unstable with respect to small perturbations. When a perturbation current, for example, spontaneously generated by a growing instability, flows along the field line on the rational surface, the flux surfaces will deform into a thin tube around the exact $q = 7$ line. Viewed in cross-section, this is an island, in the middle of the unperturbed nested magnetic surfaces. **a**, Unperturbed surfaces are shown. **b**, A magnetic island has grown around a rational field line. The flux tube associated with the island winds around the torus like the field line itself, kinking the magnetic surface it has deformed. For this reason, the instability giving rise to this deformation is called a kink instability. It is the strongest MHD instability. For the island growth process to happen, field lines have to 'reconnect', a process that needs finite plasma resistivity in the region where reconnection takes place to change the topology of the flux surfaces.

NATURE PHYSICS DOI: 10.1038/NPHYS3745

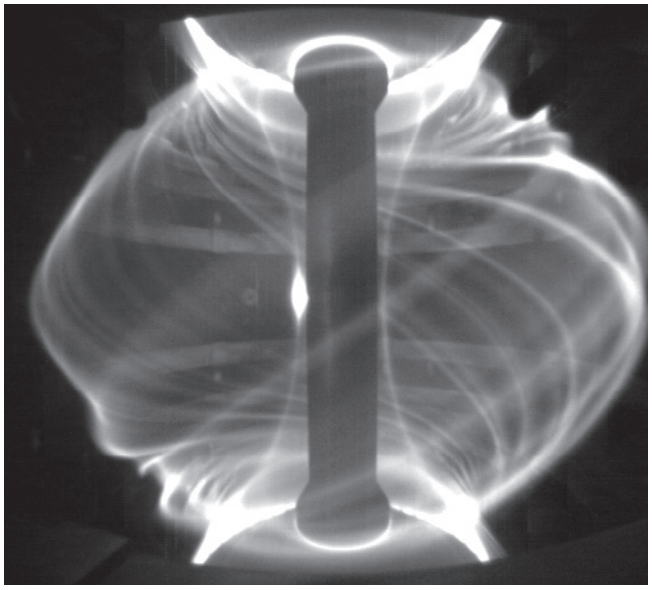

Figure 5 | Edge-localized mode (ELM) instability. Camera image of a plasma discharge in the Mega Ampere Spherical Tokamak (MAST) during an ELM instability. The plasma filaments expelled by the perturbation can be clearly seen. Figure reproduced from ref. 101, IOP.

when occurring in nonlinear limit cycles that result in quasi-stationary conditions. Examples of such self-organized cycles are the limitation of the central current density in tokamaks by the so-called 'sawtooth instability' or the regulation of the edge pressure gradient by edge-localized modes (ELMs)[28], although the latter can lead to unwanted pulsed heat loads on components. An image of a tokamak plasma taken with a fast camera during an ELM instability is shown in Fig. 5.

In recent years, our understanding of MHD stability limits to tokamak operation has advanced substantially, and it has become clear that, by appropriately shaping the pressure and current profiles of a plasma discharge, these limits can be optimized. In present-day experiments, the heating and current-drive (H&CD) systems used to heat the plasma to the necessary temperatures can be used for this purpose. In future reactors, control of the profiles via auxiliary heating systems will be much less efficient because, owing to the large self-heating by α-particles, various plasma profiles will mostly be determined by plasma self-organization. In addition to advances in tailoring stability limits, there has also been remarkable progress in actively controlling MHD instabilities once a stability boundary is crossed, using either external coils or local current drive, both of which can counteract the growth of MHD instabilities[29]. However, it remains to be assessed in future experiments whether operational scenarios requiring continuous active control are suited for reactor application or whether these methods will be used only if a stability boundary has been crossed inadvertently.

Operation at high β-values will be of special importance for steady-state operation of tokamaks. To achieve this, one has to provide a fully non-inductive current drive, because the transformer principle applied in the classical tokamak scheme is limited by the amount of flux available in the primary transformer coil. Because current drive by H&CD systems is not very efficient, one will have to rely[30] to a large extent on the bootstrap current. It has been found that to drive a substantial fraction of the total current by the bootstrap effect, operation at β-values close to the ideal MHD limit is necessary, emphasizing the need for operational scenarios that can be reliably operated under these conditions. Developing such 'advanced tokamak' scenarios is hence a focus of recent research in the context of ITER (see below) and of future demonstration (DEMO) reactors.

Finally, we note that the pressure of the fast α-particles generated by fusion reactions can also give rise to instabilities, because their density gradient also acts as a source of free energy for MHD phenomena[31]. In particular, fast particles can excite weakly damped Alfvén modes. These then lead to a redistribution of the fast particles, which might cause a reduction in heating efficiency and damage to first-wall components when they are expelled from the plasma. It is one of the major goals of ITER to study for the first time the physics of the thermonuclear burn—that is, a magnetically confined plasma with a large amount of fast α-particles (suprathermal α-particles slowing down from their 'birth energy' of 3.5 MeV with a number density of about 1% of the electron number density in the core plasma) from the fusion reaction. This is equivalent to about 66% of the plasma heating being provided by α-particles in $Q = 10$ ITER plasmas, and the processes described above could play major roles.

Power and particle exhaust and first-wall materials

The controlled exhaust of heat and particles from a fusion plasma is a central requirement for a fusion power plant (or any plasma to be kept in a steady state). Heat injected from outside the plasma as well as from the 3.5 MeV α-particles has to be exhausted to maintain a constant plasma temperature.

Deuterium and tritium must be continuously injected, as they are consumed by the fusion reaction, and once the α-particles have transferred their energy to the thermal plasma, they have to be exhausted[32]. Excessive dilution of the fusion fuel by He ash and impurities in the plasma core can cause a reduction of the reactivity of the burning fusion plasma, possibly up to extinction, in two ways: if the DT fuel density decreases too much because of the presence of He ash, the reactivity will decrease; the presence of impurities in the plasma core (especially those with a high atomic charge) leads to increased radiation losses and a subsequent decrease of the plasma temperature and reactivity. The source of fuel particles is gas puffing or (cryogenic) pellet injection; impurities enter the plasma mainly from plasma–wall interactions.

In addition to α-particles, the fusion reactions (see Box 1) produce neutrons that carry 80% of the fusion power and do not interact with the magnetic field or the plasma. Therefore, they are not part of the plasma power-and-particle balance. However, owing to the neutron irradiation, the material structures surrounding the plasma need to be made from low-activation materials (see ref. 33). Considering the deterioration of irradiated materials, and assuming present-day technology, the tolerable heat loads are below 10 MW m^{-2}. However, neutrons as a fusion product have the advantage that their power does not have to be exhausted through plasma channels. Neutrons deposit their energy much more homogeneously in the volume of a tritium-breeding blanket surrounding the plasma chamber, thus considerably reducing the requirements for the heat exhaust through plasma transport.

The magnetic-field topology of a magnetically confined plasma turns the heat and particle exhaust into a very special problem. The basis of magnetic confinement is the large anisotropy of the plasma transport, which means that, under typical fusion conditions, the transport perpendicular to the magnetic field lines is about ten orders of magnitude smaller than that parallel to the magnetic field. Whereas in the confined plasma region, with closed magnetic-flux surfaces (core plasma, indicated by solid magnetic-surface lines in Fig. 6), cross-field transport is very small, in the regions outside the closed-flux surfaces (indicated by dashed lines in Fig. 6), the open magnetic field lines connecting to wall elements result in a strong localization of heat and particle fluxes, as any plasma particle leaving the confinement region flows along the open field lines to the wall. In so-called divertor

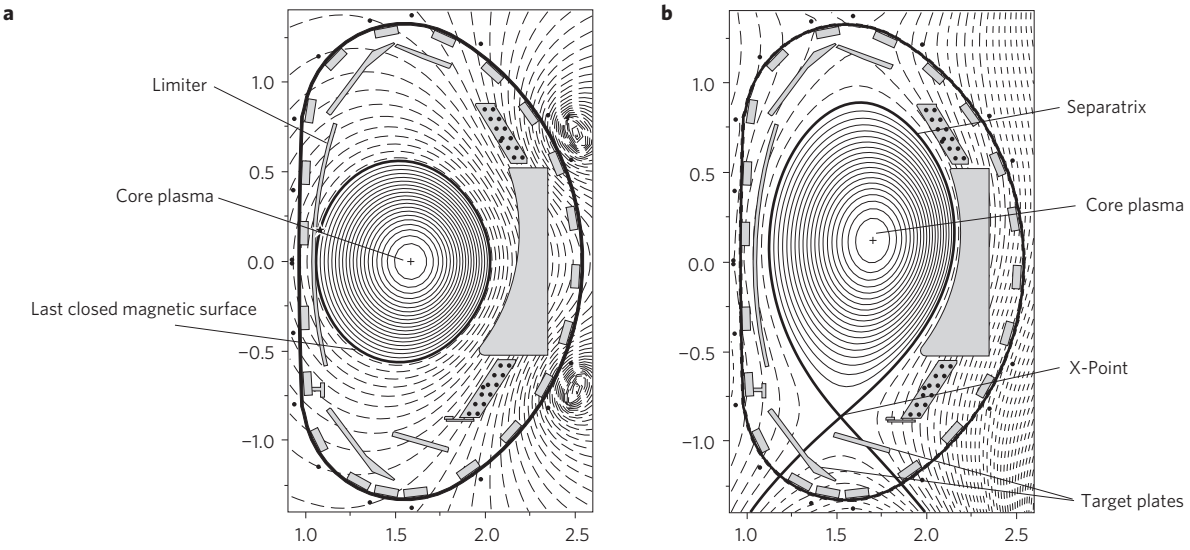

Figure 6 | Limiter and divertor configurations. Different ways to bring the plasma edge in contact with the wall. **a**, In a limiter configuration the plasma touches the first wall in the main chamber and the target plates do not play a role. **b**, In a divertor configuration the confined plasma does not touch the walls and the magnetic topology of the divertor configuration guides the edge plasma towards the target plates.

configurations (see Fig. 6b), this is realized by magnetic field topologies that direct the open field lines into remote areas which are sufficiently distant from the confined plasma and are equipped with high-heat-flux targets that can withstand the high heat and particle loads.

Typical heat flux values in the divertor of present-day experiments are of the order of 10 MW m^{-2}. This is about the upper limit of what a heat exchanger can handle, and corresponds to about 20 times the values of heat exchangers in conventional power plants. However, extrapolating to fusion power plant conditions shows that without any countermeasures—that is, simply relying on exhausting all the power from the fusion plasma through heat conduction and convection—this value will increase even further. Taking into account that the effects of the neutron irradiation on the material properties expected in a power plant actually require values below 10 MW m^{-2}, solutions have to be found to alleviate this problem. Present research focuses on three options: first, by trying to modify the magnetic-field topology in such a way that the length of the open field lines and the areas covered by them are maximized, reducing the heat flux geometrically, and by increasing the effect of the perpendicular transport of the plasma flow along these open field lines[34–39]; second, by supplying the plasma with controlled amounts of impurities, such as noble gases[40–43], that radiate in the plasma periphery and thus reduce the heat flux reaching the targets by distributing the heat more homogeneously over the inner wall of the plasma vessel; and third, by maximizing the plasma density and minimizing the plasma temperature in front of the target, so that the plasma starts to recombine, forming a neutral-gas cushion that reduces the energy of the particles impinging on the target, and at the same time leading to stronger radiation in the plasma periphery and a reduction of the heat flux[44]. At sufficiently low plasma temperatures in front of the target, the neutral pressure can actually dominate the pressure balance such that the plasma is effectively extinguished before reaching the target. This state is called 'detachment'.

The total radiation fraction envisaged for a power plant, limiting the heat flux to values below 10 MW m^{-2}, lies in the range of 90% of the heating power (the sum of the auxiliary power and the power from α-particles)[45]. It is important to note that a major fraction of this radiation must come from the plasma periphery, rather than from the core—where it would represent a heat loss and would hence lead to a lower core temperature and reduced fusion reactivity.

The choice for the materials that cover the plasma-facing components is directly linked to the heat and particle exhaust and the transport properties of the plasma. Two requirements have to be combined: material erosion has to be small enough to guarantee a sufficiently long lifetime of the most loaded components. In addition, the plasma contamination by impurities, which arises from the interplay between wall erosion and plasma transport, has to be compatible with a burning fusion plasma. In other words, the core radiation losses due to impurity ions in the plasma and the dilution of the plasma fuel have to remain low enough, such that the plasma burn is not extinguished. Following the arguments given above, however, substantial radiation is desired in the plasma periphery. Historically, carbon was used as the first-wall material in many fusion experiments because it does not melt and has a relatively high sublimation temperature. Furthermore, as a wall material, carbon is a good heat conductor and, as an impurity at fusion-relevant plasma temperatures, it is fully ionized and thus not a very effective radiator. However, the chemical interaction of carbon with a hydrogen plasma results in high erosion levels. In addition, hydrocarbon compounds are formed that redeposit in many areas of the plasma chamber. In the case of tritium, this results in a steady accumulation of tritium inside the plasma vessel, which, from a safety point of view, is not acceptable[46]. A heavy metal plasma facing material, molybdenum, has been used very early and successfully for a long time in the tokamak Alcator C-Mod[47]. After realizing the problems of carbon, alternative materials have been sought. Pioneered in the Axially Symmetric Divertor Experiment—Upgrade (ASDEX Upgrade) tokamak[48], tungsten is now regarded as a candidate material for a fusion power plant. To test the wall-material solution adopted in ITER—that is, tungsten in the divertor and beryllium for the rest of the plasma-facing components—JET has been equipped with this material composition[49]. Because of its high atomic charge, tungsten is a very effective core radiator, even at high plasma temperatures. Therefore, only very low levels of tungsten can be allowed in the plasma (10 ppm). This is achieved by the very high temperature threshold for physical sputtering of tungsten and control of the plasma transport in the core of the plasma[50]. Many fusion power plant studies assume tungsten as the material

NATURE PHYSICS DOI: 10.1038/NPHYS3745

for highly loaded components (divertor and surrounding structure) and steel for areas that are exposed only to plasma radiation[51]. However, tungsten is not yet qualified as a first-wall material to the same extent that carbon was. Tests of its mechanical durability under repeated high-heat-load pulses look promising[52]. Whether such properties will be maintained under neutron irradiation is under investigation[53]. The physics questions with respect to its compatibility with high-performance plasmas are being investigated at present in experiments[49,54].

Achievements of the worldwide fusion programme

In the early years of fusion research, a multitude of different devices and various magnetic topologies were in use: mirror machines, toroidal pinches, early stellarators and small tokamaks[3]. In the early toroidal devices, the energy confinement seemingly followed the so-called Bohm scaling for the energy-confinement time, $\tau_E \propto BR^2/T$. This predicted disappointingly low energy-confinement times, far too low for any practical realization of a fusion reactor.

However, a major breakthrough happened in 1968 on the T-3 tokamak at the Kurchatov Institute (Moscow, then USSR). It exhibited a much higher temperature (10 million °C) and a much longer energy-confinement time than any other device; values for τ_E exceeded the predictions of Bohm scaling by a factor of no less than 30. The results were announced at the memorable 1968 International Atomic Energy Agency (IAEA) Fusion Energy Conference held in Novosibirsk (then USSR). The results were later independently confirmed by a team of scientists from the Culham Laboratory, who took their measuring equipment to Moscow[55]. It resulted in a general redirection of the worldwide fusion programme towards tokamaks. The clearest example of this revolution in fusion science was the transformation of the C-Stellarator at the Princeton Plasma Physics Lab into the ST-Tokamak. The results obtained on T-3 also sparked the idea to construct a large tokamak device, to check the potential of the tokamak configuration for a future fusion power reactor. A design team to work out plans for such a large European tokamak started in 1973, leading in 1975 to the design proposal for JET[56].

A first criterion determining the quality of a fusion experiment is given by the Lawson criterion, defining the necessary conditions for ignition. For magnetic-fusion plasmas operating in the limited temperature range of a few tens or hundreds of millions °C, one can recast this inequality in the 'triple product' criterion: $n_i T_i \tau_E \geq 26 \times 10^{20}$ m^{-3} s keV, where the ion temperature T_i appears explicitly. It expresses the fact that the plasma must be contained at a sufficiently high ion pressure (proportional to $n_i T_i$) for a sufficiently long time τ_E.

Thanks to JET and other smaller tokamaks worldwide, fantastic progress has been obtained in fusion research during the past four decades. This is clearly visible from the evolution for the value of the fusion product: compared to the first tokamak experiments in the 1950s, this value has increased by a factor of more than 10,000. The results obtained on JET, the Japanese Torus 60 Upgrade (JT-60U) and the Tokamak Fusion Test Reactor have contributed significantly to this progress and, at present, values very close to break-even have been obtained in DT experiments.

An important milestone was reached in 1991 with the first production of large amounts of energy from controlled fusion reactions, with tritium being used for the first time as fuel in a tokamak[1]. These experiments, obtained with a mixture of 90% D and 10% T, generated fusion powers in the megawatt range for nearly 2 s, with a maximum of about 1.7 MW (corresponding to a Q value of about 0.15). Further success was obtained early in 1994 on the TFTR tokamak. In plasmas consisting of a mixture of 50% deuterium and 50% tritium, multi-megawatt-level fusion powers were generated for about one second, with a maximum of 6.3 MW (refs 57,58), and plasma temperatures in excess of 300 million °C were reached in the plasma centre, 20–30 times hotter than the centre of the Sun. In November 1994, fusion powers of more than 10 MW were generated, corresponding to Q values of about 0.27 (ref. 59). Further record values were reached in 1996 on the JT-60U tokamak. This machine demonstrated temperatures in excess of 520 million °C (ref. 60), the highest temperature ever realized in a controlled way in macroscopic volumes on Earth. Even more important, a record value for the fusion triple product was obtained in pure deuterium plasmas. If the same conditions had been realized in DT plasmas, it would have resulted in a Q value of about 1.25—that is, above break-even[61].

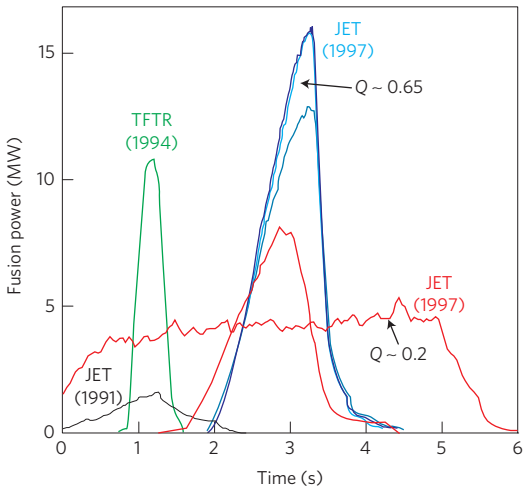

Figure 7 | Deuterium–tritium fusion records. Shown are the time evolutions of the measured fusion power output in historical DT experiments in TFTR and JET[63]. Q-values shown here are conservative. In transient pulses, such as the record 16.1 MW one, part of the injected power goes into building up the plasma's internal energy and not into sustaining the fusion reactions. Correcting for this effect, Keilhacker *et al.*[62] have estimated that the equivalent stationary Q-value for this pulse would be 0.94 (rather than 0.65 as shown in the figure). In addition, these experiments also provided a first glimpse at the effects on the plasma of fast α-particles. Indeed, with their energy of 3.5 MeV they can trigger various instabilities (for example, Alfvén eigenmodes); they are absent in all non-DT tokamak-experiment plasmas, thus such effects could not be studied before. Figure reproduced from ref. 63, IOP.

The most impressive results with DT plasmas in fusion research were obtained in JET, in October and November 1997. Experiments with 50% D/50% T plasmas resulted in over 16 MW of fusion power lasting about 1 s, with Q values of about 0.65 (ref. 62). Correcting for transient effects, the equivalent steady-state Q becomes 0.94. These are the highest fusion powers and Q values so far reached, thereby effectively nearing a first demonstration of break-even in reactor-grade DT fusion plasmas. A quasi-steady-state generation of fusion power has also been demonstrated: over 4 MW of fusion power was produced for time intervals of more than 5 s (ref. 63), a duration limited only by the technical constraints of JET. An overview of the various DT experiments is shown in Fig. 7.

However, from the above discussion one should not get the impression that the stellarator concept is not a valid candidate for a fusion reactor. Compared to the results of the early years, confinement times have now increased by a factor of 100. This is still a factor of 10 below that of tokamaks. As mentioned before, stellarators have the intrinsic advantage of very long pulses. Equipped with superconducting coils, they enable one to study the effects of the very long time constants involved in the interaction between the hot plasma and the first wall. This is illustrated by recent results obtained on the LHD. Pulses with a duration of

about 50 min on this device demonstrate the principal advantage of the steady-state magnetic-confinement concept[64]. Further steps forward are expected from the superconducting stellarator W7-X. Whereas the unperturbed magnetic field of tokamaks is axially symmetric, stellarators generally do not possess such a continuous symmetry[22,65]. The design of W7-X is based on an elaborate optimization procedure[66,67]. Relying on extensive computer codes, W7-X is also a result of the rapid development of supercomputers.

Finally, we would like to note that, although the ultimate goal of fusion research is the realization of a viable fusion power plant, this on-going pursuit has led to fundamental discoveries in plasma physics outside the context of fusion—see, for example, ref. 68.

ITER

The ITER project was officially launched in 2006 as a joint venture between the European Union, India, Japan, Korea, Russia and the US . Hosts are Europe and France; the construction site is next to the CEA's Cadarache research centre[69].

The main objective of ITER is to demonstrate the feasibility of a burning fusion plasma, which is characterized by a significant fraction of α-particle heating maintained over 10 min (ref. 70). At a power amplification of $Q = 10$, the heating power from α-particles, given by the ratio $Q/(Q + 5)$, constitutes two thirds of the total heating power. Such a α-heating fraction is not only quantitatively but also qualitatively different from previous DT experiments. Physics constraints, given by the confinement properties and the stability boundaries of the plasma, result in a fusion power of 500 MW, with 20% delivered to the thermal plasma by collisional transfer from the 3.5 MeV α-particles resulting from the fusion reactions. For comparison, in the DT experiments on JET in 1997 the achieved fusion power was much lower (about 16 MW), and the contribution of the α-particles to the heating of the plasma at $Q \approx 1$ about 15%. In future ITER experiments, the degree of self-organization will be much larger than in present experiments, where the heating power deposition is to a large extent an externally adjusted quantity. In addition, it will become possible to study the role of collective effects of the fast ions on the plasma behaviour, such as α-driven instabilities[71]. Another important objective of ITER is to study concepts for tritium breeding from lithium, using the fast neutrons of the DT reaction. For this purpose, ITER will be equipped with different types of test blanket modules[72].

Although ITER is still an experimental device, its design and construction are unprecedented. From an engineering point of view, although not yet a power plant, the size and complexity of ITER are indeed challenging: a magnetic-field volume of $\sim$840 m^3 with magnetic fields on the torus axis close to 6 T and up to 12 T at the coils, requiring specially developed superconductors[73] together with an elaborate mechanical support structure; negative-ion-beam plasma-heating sources for the injection of fast neutral atoms with energies up to 1 MeV (ref. 74); radio frequency auxiliary heating systems[75–77]; complex plasma control for operational scenarios and protection of the device. Every effort is being undertaken to make all this reliably work together. The use of tritium and the activation of the plasma vessel and components inside the plasma vessel requires a remote-handling system for handling those components[78,79] and demands a dedicated safety concept with a special licensing procedure. Plans, which will be refined in the coming years, have been devised for the disposal in several phases of the nuclear waste left at decommissioning[80,81].

From the physics point of view, besides the goal of a burning fusion plasma, the most challenging scientific problems that must be overcome in ITER are threefold. The first is the handling of the energy and particle exhaust from the plasma in conditions not experienced so far in fusion experiments. This pertains to the issue of the plasma-facing components and, in particular, that of the divertor, as discussed above. The second is the control and mitigation of ELMs. The third is the avoidance or mitigation of the most detrimental instability, the disruption.

An ELM is a burst of energy expelled from the plasma. The ELMs appear in Fig. 5 as a filamentary bright structure. Such structures periodically become unstable and are expelled radially; the associated power flux is partly transported to the divertor (along or near the last closed-flux magnetic surface) and to some extent deposited on the plasma-facing components. In ITER, there can be several hundreds of ELMs per plasma pulse, leading to energy fluxes on the plasma-facing components that can reach 1 MJ m^{-2} on a sub-millisecond timescale. This could lead to unacceptable erosion (or melting or vaporization) of plasma-facing components, thereby reducing their lifetime and making them a possible source of impurities. Mitigation of ELMs can be done by means of periodic pellet injection, which increases the ELM frequency but reduces the amount of energy expelled per ELM. ELMs can also be suppressed by using magnetic perturbation coils that cause a modification of the magnetic-field configuration in the region of the H-mode transport barrier preventing the growth of ELM instabilities[82]. Such coils will be available in ITER[83]. Work on extrapolation of results obtained on present machines to a large burning plasma remains the subject of ongoing research at facilities such as the tokamak DIII-D[84].

A major disruption usually starts with magnetic-reconnection events affecting the whole plasma cross-section and resulting in transport of cold plasma to the hot plasma centre. The plasma temperature decays while its thermal energy is transported to the periphery (thermal quench phase) on a millisecond timescale. As the central plasma conductivity drops, the plasma current is first redistributed over the plasma cross-section, and afterwards onto the vacuum vessel, as the plasma has nearly totally lost its conductivity (current quench phase).

In vertically elongated plasmas, the magnitude of the currents in parts of the vessel structure can be increased by a vertical displacement caused by the coupling of the unstable helical mode in the plasma and initial up–down asymmetries of the magnetic configuration. These are called vertical displacement events (VDEs). During the current quench phase, part of the current may be transferred to 'runaway' electrons. These are generated when the plasma density is low and collisions with other particles become ineffective. The result is that the electrons are continuously accelerated (up to relativistic energies) by the toroidal electric field around the plasma ring induced by the transformer. Runaway electrons are more easily generated in large machines operated at higher magnetic fields, and in the case of ITER could attain up to 70% of the plasma current[70]. Runaway electrons can also be generated in other situations such as intentional fast-plasma shutdowns and disruptions. Having large energies, they can cause considerable damage when colliding with plasma-facing components.

Disruptions should generally be avoided. From the structural point of view, at each disruption all components of the vacuum vessel—mainly plasma-facing components and structural parts—are subject to huge transient forces. Although in ITER these machine parts have been designed to withstand such forces, repeated disruptions will cause fatigue. Hence, only a limited number of disruptions can be tolerated. The second negative aspect of disruptions is the increased thermal stress of plasma-facing components during the thermal quench phase, where most of the kinetic energy of the plasma is expelled to first-wall structures in milliseconds. Mechanical effects of disruptions can be mitigated by reducing the image currents (especially during VDE events) in electrically conducting first-wall structures by a shift of the plasma position or by impurity injection quickly after the detection of the thermal quench phase. Thermal effects can be mitigated by massive impurity (usually noble-gas) injection that converts part

of the plasma thermal energy into radiation. Preventing the build-up of intense runaway electron beams requires an increase of the electron density, as this provides the most effective brake to electron acceleration. This can also be realized by massive injection (some 10^{22} atoms injected in a few tens of milliseconds) or pellet injection of impurities or hydrogen. The choice of mitigation strategies for ITER is an active field of research[85].

DEMO and future fusion reactors

As shown in the previous section, ITER will demonstrate the feasibility of sustaining a magnetically confined thermonuclear plasma with dominant self-heating by the α-particles generated in the fusion reaction. However, ITER is not designed to generate electricity from the heat produced by the fusion reaction because, on the one hand, its power amplification of $Q = 10$ is not sufficient to generate net electricity, assuming the usual thermodynamic efficiency of around 35% for power conversion, and, on the other hand, it is being designed as an experimental device—it will run at low-duty cycle, that is, the time in between the discharges will be much longer than the duration of the discharges. For this reason, ITER will also not breed the tritium required for the plasma burn, but will test tritium breeding in dedicated first-wall panels, each using a different breeding technology, in preparation of a DEMO reactor for which a tritium-breeding blanket will be needed.

Concerning fusion plasma physics, the operational mode in DEMO will hence differ from ITER because very long pulses or stationary operation are required and the plasma should have a substantially higher Q, of the order of 30–50, to be able to produce electricity in an economical way. Applying the scaling law used for predicting the energy-confinement time in ITER, it turns out that a tokamak DEMO reactor will have to be bigger, but not by much. Present designs foresee a major radius R_0 in the range 7–9 m (the major radius of ITER is 6.2 m), which should be sufficient to provide the high Q (ref. 86). However, substantially increasing the fusion power implies operation at higher β, roughly double the ITER value—that is, close to the β-limit discussed previously. Such high values are also required to increase the pulse length towards steady state owing to the above-mentioned increase of the pressure-driven bootstrap current. Development of an 'advanced tokamak' scenario is hence of great importance for the step from ITER to DEMO.

A substantial part of DEMO research is planned at the Japanese Tokamak 60 Super Advanced (JT-60SA, the successor of JT-60U)[87,88], at present under construction in the context of the Broader Approach Agreement between Europe and Japan. JT-60SA is designed for studying fully non-inductive steady-state operations—that is, plasmas without any transformer-induced plasma current. At plasma currents of 2.3 MA, fully non-inductively current-driven operation should be possible at β values nearly twice those of ITER ($\beta_N = 4.3$) with a total additional heating power of 37 MW. The adopted strategy is that the nonlinear optimization of the steady-state tokamak scenario for DEMO is done in JT-60SA, being more flexible than ITER, and then later confirmed with substantial heating by α-particles ($Q = 5$ scenario) in ITER.

Because the ion temperature in ITER will already be in the range of the optimum for the fusion reaction, the increase in pressure mostly has to come from an increase in plasma density, which then also puts the operational point closer to the maximum achievable density. However, we note that the density limit in tokamaks, although empirically well-established, is not understood from first principles—leaving the possibility that ways may be found for exceeding this limit if it turns out not to be a 'hard' physical limit. In fact, recent experiments indicate that a higher density can be obtained by operating with peaked density profiles, and theory predicts that, at the low collisionality prevailing under DEMO conditions, such profiles may occur naturally owing to the existence of a turbulent inward pinch velocity for particles[89]. (The so-called normalized collisionality measures how many Coulomb collisions a particle undergoes while completing a typical orbit in a torus. It will be much below unity under typical fusion conditions in ITER and DEMO.) These theoretical predictions can, however, only be verified in ITER, as none of the present experimental devices can obtain the low collisionality typical for ITER and DEMO at high density.

If DEMO were to be a stellarator device, it would inherently be steady state, because there is no need for a toroidal plasma current, as stated above. This is a considerable advantage compared to a tokamak-type DEMO reactor. Also, experimentally it has been established that the achievable density in stellarators can be much higher than that in tokamaks, a second big advantage (that yet still has to be experimentally demonstrated for reactor conditions). However, also here, there is no first-principles understanding of the density limit in stellarators, so extrapolations of experimental observations in present devices exhibit a considerable uncertainty. A third substantial advantage of stellarators is the absence of disruptions. The penalty for these advantages is a more complicated superconducting coil system that constrains access to the machine, which for example becomes an issue in the context of breeding blanket modules. Owing to the more complex geometry, it is at present not clear if the maintenance scheme for a stellarator power plant will be more difficult than that for a tokamak. However, first comparative studies indicate that the cost of stellarator and tokamak power plants are of the same order[90].

Perspectives of fusion in a future energy landscape

The foreseen solution to climate change is mainly aiming at transforming the electricity production from fossil fuels and nuclear fission into a system dominated by wind turbines and solar energy. In this context, nuclear fusion could very well become a major player, having as final aim an electricity-producing reactor[91]: it could serve as a carbon-free large-scale backup electricity system to cover dark and windstill periods in a system dominated by intermittent energy from wind and the Sun.

Fusion promises to be a long-term source of energy. Current reserves of deuterium and Li are enough to guarantee thousands of years of energy consumption at the present rate[91–94]. Construction materials for superconducting cables seem to be abundant: the estimate for world reserves of Nb is about 490 million tonnes—about 560 tonnes of Nb are required for superconducting coils in ITER (correspondence from ITER to the Tantalum-Niobium International Study Center of 8 June 2015). ^{4}He as a coolant is relatively scarce; however, much more ^{4}He could (and should) be made available, for example, with additional investments in the gas industry[95,96]—not only for fusion. Future possible advances in high-T_c superconductor materials would be advantageous (eliminating the need for Nb and enabling the use of coolants other than ^{4}He, for example, liquid nitrogen). The widely available fuel resources for fusion would also help to reduce energy dependencies in the world, an important factor contributing to a more peaceful world.

Fusion has particularly benign environmental and safety properties. The basic fuels (D and ^{6}Li) are non-radioactive, abundantly available, cheap to produce and the consumption is minimal (see Box 1). The fusion product is ^{4}He, a non-radioactive, chemically inert substance, not contributing to climate change. In addition, unlike nuclear fission, where the reactor contains sufficient fuel for several months of operation, a magnetic-fusion device contains only tiny quantities (a few gram) of fuel needed for its operation during the next few seconds. Thus, in the case of any malfunction, cutting the fuel supply immediately stops the fusion burning process. If, by accident, the hot plasma were to touch the wall, any tiny amount of evaporated material would radiate away (onto the machine walls) the energy contained within the plasma and cool it down to temperatures where no fusion reaction

can occur. Similarly, any tiny air leak in the vacuum vessel would stop the reaction. There is no possibility of a reactor melt-down, and numerous studies show that a fusion power plant can be operated with minimal radiological risks for the environment in its immediate vicinity: the quantities of tritium released in the event of a major incident are very small[97,98]. In routine operation and maintenance, reactor operators will, of course, need to carefully avoid any tritium seepage. In contrast to nuclear fission, fusion does not raise proliferation concerns, none of the materials required being subject to the provisions of non-proliferation treaties.

Activation of the components that are bombarded by the high flux of 14.1 MeV fusion neutrons (10^{18} neutrons $cm^{-2}\,s^{-1}$ for a reactor of about 1 GW electrical power) cannot be avoided. As discussed in ref. 33, developing suitable materials that minimize swelling, embrittlement and activation effects is necessary for an economical exploitation of the inherent advantages of fusion as an energy source.

As the existing neutron sources (fission reactors, spallation sources or accelerator-driven systems) all produce neutron energy spectra that are very different from those expected in a fusion reactor, a dedicated laboratory is needed for mimicking the high flux of 14.1 MeV neutrons projected for DEMO. Such a laboratory has long been a major pending step, but spectacular progress has been reached over the past ten years, under the Broader Approach Agreement between Japan and Europe, in developing prototypes of those parts that are technologically challenging to validate their stable operation. Prototype versions of all major components have been successfully operated, pending the validation of the required deuteron accelerator, the installation and commissioning of which is progressing in Rokkasho, Japan[33]. The construction time of such a dedicated fusion materials lab is at present estimated as about eight years[99]. If a decision on location and start of construction is reached soon, obtaining first results for various fusion-reactor materials in the second half of the next decade seems a reality.

Although, at the time of decommissioning, the initial activity level of a future fusion reactor is expected to be similar to that of a fission plant, recent fusion power plant conceptual studies[51] show that the radiotoxicity using low-activation first-wall and structural materials decays by a factor of 10,000 over 100 years. After that timespan, these materials can then be regarded as non-radioactive (contact dose rate lower than 0.001 mSv h^{-1}, decay heat lower than 1 W m^{-3}) or recyclable (contact dose rate lower than 20 mSv h^{-1}, decay heat lower than 10 W m^{-3}), although recycling of some materials might require remote-handling procedures. There should therefore be no need for long-term geological repositories, and the activated material from fusion power stations would not constitute a waste-management burden for future generations.

Received 8 December 2015; accepted 22 March 2016; published online 3 May 2016; corrected after print 16 June 2016

References

1. Rebut, P.-H. *et al*. The JET preliminary tritium experiment. *Plasma Phys. Control. Fusion* **34,** 1749–1758 (1992).
2. Giruzzi, G. *et al*. Modelling of pulsed and steady-state DEMO scenarios. *Nucl. Fusion* **55,** 073002 (2015).
3. Clery, D. *A Piece of the Sun. The Quest for Fusion Energy* (Overlook Duckworth, 2013).
4. Francis, F. C. *An Indispensible Truth. How Fusion Power Can Save The Planet* (Springer, 2011).
5. Dean, S. O. *Search for the Ultimate Energy Source: A History of the U.S. Fusion Energy Program* (Springer, 2013).
6. Mazon, D., Fenzi, C. & Sabot, R. As hot as it gets. *Nature Phys.* **12,** 14–17 (2016).
7. Porkolab, M. RF heating and current drive in magnetically confined plasma: a historical perspective. *AIP Conf. Proc.* **933,** 3 (2007).
8. Lawson, J. D. *Some Criteria for a Useful Thermonuclear Reactor* (Atomic Energy Research Establishment, 1955).
9. Lawson, J. D. Some criteria for a power producing thermonuclear reactor. *Proc. Phys. Soc. B* **70,** 6–10 (1957).
10. Goldston, R. J. Energy confinement scaling in Tokamaks: some implications of recent experiments with Ohmic and strong auxiliary heating. *Plasma Phys. Control. Fusion* **26,** 87–103 (1984).
11. Kaye, S. M. & Goldston, R. J. Global energy confinement scaling for neutral-beam-heated tokamaks. *Nucl. Fusion* **25,** 65–69 (1985).
12. Ryter, F. *et al*. Electron heat transport studies. *Plasma Phys. Control. Fusion* **48,** B453–B463 (2006).
13. Wagner, F. *et al*. Regime of improved confinement and high beta in neutral-beam-heated divertor discharges of the ASDEX tokamak. *Phys. Rev. Lett.* **49,** 1408–1412 (1982).
14. Bickerton, R. J., Connor, J. W. & Taylor, J. B. Diffusion driven plasma currents and bootstrap tokamak. *Nature* **229,** 110–112 (1971).
15. Balescu, R. *Transport Processes in Plasmas* Vol. 2 (Elsevier, 1988).
16. Fasoli, A. *et al*. Computational challenges in magnetic-confinement fusion physics. *Nature Phys* **12,** 411–423 (2016).
17. Gusakov, E. Z. *et al*. Anomalous transport and multi-scale drift turbulence dynamics in tokamak ohmic discharge as measured by high resolution diagnostics and modeled by full-f gyrokinetic code. *Plasma Phys. Control. Fusion* **55,** 124034 (2013).
18. Dumont, R. J. *et al*. Interplay between fast ions and turbulence in magnetic fusion plasmas. *Plasma Phys. Control. Fusion* **55,** 124012 (2013).
19. Pace, D. C. *et al*. Keeping fusion plasmas hot. *Phys. Today* **68**(10), 34–39 (2015).
20. Howard, N. T. *et al*. Multi-scale gyrokinetic simulation of tokamak plasmas: enhanced heat loss due to cross-scale coupling of plasma turbulence. *Nucl. Fusion* **56,** 014004 (2016).
21. Staebler, G. M. & Groebner, R. J. H-mode transitions and limit cycle oscillations from mean field transport equations. *Plasma Phys. Control. Fusion* **57,** 014025 (2015).
22. Helander, P. Theory of plasma confinement in non-axisymmetric magnetic fields. *Rep. Prog. Phys.* **77,** 087001 (2014).
23. Xanthopoulos, P. *et al*. Nonlinear gyrokinetic simulations of ion-temperature-gradient turbulence for the optimized Wendelstein 7-X Stellarator. *Phys. Rev. Lett.* **99,** 035002 (2007).
24. Proll, J. H. E. *et al*. Resilience of quasi-isodynamic stellarators against trapped-particle instabilities. *Phys. Rev. Lett.* **108,** 245002 (2012).
25. Zohm, H. *Magnetohydrodynamic Stability of Tokamaks* (Wiley, 2015).
26. Troyon, F. *et al*. MHD-Limits to plasma confinement. *Plasma Phys. Control. Fusion* **26,** 209–215 (1984).
27. Greenwald, M. *et al*. A new look at density limits in tokamaks. *Nucl. Fusion* **28,** 2199–2207 (1988).
28. Zohm, H. Edge Localized Modes (ELMs). *Plasma Phys. Control. Fusion* **38,** 105–128 (1996).
29. Igochine, V. (ed.) *Active Control of MHD Instabilities in Hot Plasmas* (Springer, 2015).
30. Peeters, A. G. The bootstrap current and its consequences. *Plasma Phys. Control. Fusion* **42,** B231–B242 (2000).
31. Gorelenkov, N. *et al*. Energetic particle physics in fusion research in preparation for burning plasma experiments. *Nucl. Fusion* **54,** 125001 (2014).
32. McCracken, G. & Stott, P. *Fusion, the Energy of the Universe* (Elsevier, 2005).
33. Knaster, J., Moeslang, A. & Muroga, T. Materials research for fusion. *Nature Phys.* **12,** 424–434 (2016).
34. Kotschenreuther, M. *et al*. On heat loading, novel divertors, and fusion reactors. *Phys. Plasmas* **14,** 072502 (2007).
35. Valanju, P. M. *et al*. Super-X divertors and high power density fusion devices. *Phys. Plasmas* **16,** 056110 (2009).
36. Ryutov, D. D. Geometrical properties of a snowflake divertor. *Phys. Plasmas* **14,** 064502 (2007).
37. Pericoli, V. *et al*. Preliminary 2D code simulation of the quasi-snowflake divertor configuration in the FAST tokamak. *Fusion Eng. Des.* **88,** 1671–1681 (2013).
38. Ryutov, D. D. *et al*. A snowflake divertor: a possible solution to the power exhaust problem for tokamaks. *Plasma Phys. Control. Fusion* **54,** 124050 (2012).
39. Ryutov, D. D. & Umansky, M. Divertor with a third-order null of the poloidal field. *Phys. Plasmas* **20,** 092509 (2013).
40. Winter, J. *et al*. Improved plasma performance in TEXTOR with silicon coated surfaces. *Phys. Rev. Lett.* **71,** 1549–1552 (1993).
41. Gruber, O. *et al*. Observation of continuous divertor detachment in H-mode discharges in ASDEX Upgrade. *Phys. Rev. Lett.* **74,** 4217–4220 (1995).

42. Messiaen, A. *et al*. High confinement and high density with stationary plasma energy and strong edge radiation in the TEXTOR-94 tokamak. *Phys. Rev. Lett.* **77,** 2487–2490 (1996).
43. Ongena, J. *et al*. Experiments with radiative mantle plasmas. *Fusion Sci. Technol.* **53,** 943–952 (2008).
44. Umansky, M. V. *et al*. Analysis of geometric variations in high-power tokamak divertors. *Nucl. Fusion* **49,** 075005 (2009).
45. Kallenbach, A. *et al*. Impurity seeding for tokamak power exhaust: from present devices via ITER to DEMO. *Plasma Phys. Control. Fusion* **55,** 124041 (2013).
46. Federici, G. *et al*. Plasma-material interactions in current tokamaks and their implications for next step fusion reactors. *Nucl. Fusion* **41,** 1967–2137 (2001).
47. Greenwald, M. *et al*. 20 years of research on the Alcator C-Mod tokamak. *Phys. Plasmas* **21,** 110501 (2014).
48. Neu, R. *et al*. The tungsten divertor experiment at ASDEX Upgrade. *Plasma Phys. Control. Fusion* **38,** A165–A179 (1996).
49. Romanelli, F. *et al*. Overview of JET results. *Nucl. Fusion* **55,** 104001 (2015).
50. Höhnle, H. *et al*. Extension of the ECRH operational space with O2 and X3 heating schemes to control tungsten accumulation in ASDEX Upgrade. *Nucl. Fusion* **51,** 083013 (2011).
51. Maisonnier, D. *et al*. Power plant conceptual studies in Europe. *Nucl. Fusion* **47,** 1524–1532 (2007).
52. Seki, Y. *et al*. in *Proc. 25th IAEA Fusion Energy Conf.* FIP/1-1. (IAEA, 2014).
53. Hasegawa, A. *et al*. in *Proc. 25th IAEA Fusion Energy Conf.* MPT/1-4 (IAEA, 2014).
54. Zohm, H. for the ASDEX Upgrade Team and the EUROfusion MST1 Team Recent ASDEX Upgrade research in support of ITER and DEMO. *Nucl. Fusion* **55,** 104010 (2015).
55. Peacock, N. J. *et al*. Measurement of the electron temperature by Thomson scattering in tokamak T3. *Nature* **224,** 488–490 (1969).
56. Rebut, P. H. *et al*. *JET Project – Design Proposal* EUR-JET-R5 (Commission of the European Communities, 1975).
57. Strachan, J. *et al*. Fusion power production from TFTR plasmas fueled with deuterium and tritium. *Phys. Rev. Lett* **72,** 3526–3529 (1994).
58. Hawryluk, R. J. *et al*. Confinement and heating of a deuterium–tritium plasma. *Phys. Rev. Lett.* **72,** 3530–3533 (1994).
59. McGuire, K. M. *et al*. Review of deuteriumtritium results from the Tokamak Fusion Test Reactor. *Phys. Plasmas* **2,** 2176–2188 (1995).
60. Ishida, S. *et al*. in *Proc. 16th IAEA Conference on Fusion Energy* Vol. 1, 315–330 (IAEA, 1997).
61. Fujita, T. *et al*. High performance experiments in JT-60U reversed shear discharges. *Nucl. Fusion* **39,** 1627–1636 (1999).
62. Keilhacker, M. *et al*. High fusion performance from deuterium-tritium plasmas in JET. *Nucl. Fusion* **39,** 209–234 (1999).
63. Jacquinot, J. & the JET Team Deuterium-tritium operation in magnetic confinement experiments: results and underlying physics. *Plasma Phys. Control. Fusion* **41,** A13–A46 (1999).
64. Tokitani, M. *et al*. Plasma wall interaction in long-pulse helium discharge in LHD Microscopic modification of the wall surface and its impact on particle balance and impurity generation. *J. Nucl. Mater.* **463,** 91–98 (2015).
65. Helander, P. *et al*. Stellarator and tokamak plasmas: a comparison. *Plasma Phys. Control. Fusion* **54,** 124009 (2012).
66. Grieger, G. *et al*. Physics optimization of stellarators. *Phys. Fluids B* **4,** 2081–2091 (1992).
67. Bosch, H.-S. *et al*. Technical challenges in the construction of the steady-state stellarator Wendelstein 7-X. *Nucl. Fusion* **53,** 126001 (2013).
68. Melnikov, A. V. Applied and fundamental aspects of fusion science. *Nature Phys.* **12,** 386–390 (2016).
69. Interview with Bernard Bigot: building the way to fusion energy. *Nature Phys.* **12,** 395–397 (2016).
70. Progress in ITER Physics Basis. *Nucl. Fusion* **47**, S1–S414 (2007); corrigendum **48**, 099801 (2008).
71. Vlad, G. *et al*. Alfvéic instabilities driven by fusion generated alpha particles in ITER scenarios. *Nucl. Fusion* **46,** 1–16 (2006).
72. Giancarli, L. M. *et al*. Overview of the ITER TBM Program. *Fusion Eng. Des.* **87,** 395–402 (2012).
73. Sborchia, C. *et al*. The ITER magnet systems: progress on construction. *Nucl. Fusion* **54,** 013006 (2014).
74. Toigo, V. *et al*. in *Proc. 25th IAEA Fusion Energy Conf.* FIP/2-4Rc (IAEA, 2014).
75. Wilson, J. R. & Bonoli, P. T. Progress on ion cyclotron range of frequencies heating physics and technology in support of the International Tokamak Experimental Reactor. *Phys. Plasmas* **22,** 021801 (2015).
76. Omori, T. *et al*. Overview of the ITER EC H&CD system and its capabilities. *Fusion Eng. Des.* **86,** 951–954 (2011).
77. Hoang, G. T. *et al*. A lower hybrid current drive system for ITER. *Nucl. Fusion* **49,** 075001 (2009).
78. Motojima, O. The ITER project construction status. *Nucl. Fusion* **55,** 104023 (2015).
79. Buckingham, R. & Loving, A. Remote-handling challenges in fusion research and beyond. *Nature Phys.* **12,** 391–393 (2016).
80. *Summary of the ITER Final Design Report* Ch. 8 (IAEA, 2001).
81. Pampin, R. *et al*. Activation analyses updating the ITER radioactive waste assessment. *Fusion Eng. Des.* **87,** 1230–1234 (2012).
82. Hill, D. N. & the DIII-D team. DIII-D research towards resolving key issues for ITER and steady-state tokamaks. *Nucl. Fusion* **53,** 104001 (2013).
83. Encheva, A. *et al*. in *Proc. 25th IAEA Fusion Energy Conf.* FIP/1-5 (IAEA, 2014).
84. Buttery, R. J. & the DIII-D team. DIII-D research to address key challenges for ITER and fusion energy. *Nucl. Fusion* **55,** 104017 (2015).
85. Baylor, L. R. *et al*. in *Proc. 25th IAEA Fusion Energy Conf.* FIP/2-1 (IAEA, 2014).
86. Zohm, H. On the minimum size of DEMO. *Fus. Sci. Technol.* **58,** 613–624 (2010).
87. Ishida, S., Barabaschi, P., Kamada, Y. & the JT-60SA Team Overview of the JT-60SA project. *Nucl. Fusion* **51,** 094018 (2011).
88. Barabaschi, P. *et al*. in *Proc. 25th IAEA Fusion Energy Conf.* OV/3-2 (IAEA, 2014).
89. Angioni, C. *et al*. Density peaking, anomalous pinch, and collisionality in tokamak plasmas. *Phys. Rev. Lett.* **90,** 205003 (2003).
90. Warmer, F. System code analysis of helias fusion reactor and economic comparison to tokamaks. *IEEE Trans. Plasma Sci.* http://dx.doi.org/10.1109/TPS.2016.2545868 (2016).
91. Cowley, S. C. The quest for fusion power. *Nature Phys.* **12,** 384–386 (2016).
92. *Mineral Commodities Summaries* (US Geological Survey, 2015); http://minerals.usgs.gov/minerals/pubs/mcs/2015/mcs2015.pdf
93. Evans, R. K. An Abundance of Lithium (North Carolina State University, 2008); http://www.che.ncsu.edu/ILEET/phevs/lithium-availability/An_Abundance_of_Lithium.pdf
94. Evans, R. K. An Abundance of Lithium Part Two (EV World, 2008); http://www.evworld.com/library/KEvans_LithiumAbunance_pt2.pdf
95. Nuttal, W. J., Clarke, R. H. & Glowacki, B. A. Stop squandering helium. *Nature* **485,** 573–575 (2012).
96. Peterson, J. B. in *The Future of Helium as a Natural Resource* (eds Nuttall, W. J., Clarke, R. & Glowacki, B. A.) 48–54 (Routledge, 2012).
97. *A Conceptual Study of Commercial Fusion Power Plants*; (European Fusion Development Agreement, 2005); https://www.euro-fusion.org/wpcms/wp-content/uploads/2012/01/PPCS_overall_report_final-with_annexes.pdf
98. *Safety and Environmental Impact of Fusion* (European Fusion Development Agreement, 2001); https://www.euro-fusion.org/wpcms/wp-content/uploads/2012/01/SEIF_report_25Apr01.pdf
99. Knaster, J. *et al*. IFMIF, the European-Japanese efforts under the Broader Approach Agreement towards a Li(d,xn) neutron source: current status and future options. *Nucl. Mater. Energy* (in the press).
100. Gusev, V. K., Alladio, F. & Morris, A. W. The basics of spherical tokamaks and progress in European research. *Plasma Phys. Control. Fusion* **45,** A59–A82 (2003).
101. Kirk, A. *et al*. Structure of ELMs in MAST and the implications for energy deposition. *Plasma Phys. Control. Fusion* **47,** 315 (2005).

Acknowledgements

J.O. and R.K. have the great pleasure to thank M. Van Schoor for pertinent valuable advice and discussions when writing this Review.

Additional information

Reprints and permissions information is available online at www.nature.com/reprints. Correspondence should be addressed to J.O.

Competing financial interests

The authors declare no competing financial interests.

Erratum: Magnetic-confinement fusion

J. Ongena, R. Koch, R. Wolf and H. Zohm

Nature Physics **12,** 398–410 (2016); published online 3 May 2016; corrected after print 16 June 2016.

In the version of this Review Article originally published, it was not acknowledged that Fig. 3a is courtesy of C. Brandt, IPP. This has been corrected in the online versions 16 June 2016.